Proceedings of PVP2007
2007 ASME Pressure Vessels and Piping Division Conference
July 22-26, 2007, San Antonio, Texas

PVP2007-26544

Transformation Temperatures and Welding Residual Stresses in Ferritic Steels

J. A. Francis
School of Materials
University of Manchester,
Grosvenor Street, Manchester M1 7HS, U.K.

H. J. Stone
Materials Science and Metallurgy
University of Cambridge,
Pembroke Street, Cambridge CB2 3QZ, U.K.

S. Kundu
Materials Science and Metallurgy
University of Cambridge,
Pembroke Street, Cambridge CB2 3QZ, U.K.

R. B. Rogge
Canadian Neutron Beam Centre
National Research Council, Canada
Chalk River Laboratories,
Chalk River, Ontario KOJ 1PO, Canada

H. K. D. H. Bhadeshia
Materials Science and Metallurgy
University of Cambridge,
Pembroke Street, Cambridge CB2 3QZ, U.K.

P. J. Withers
School of Materials
University of Manchester,
Grosvenor Street, Manchester M1 7HS, U.K.

L. Karlsson
ESAB AB, Central Research Laboratories
Hekulesgatan 72, Box 8004,
40277 Gothenburg, Sweden

ABSTRACT

Residual stress in the vicinity of a weld can have a large influence on structural integrity. Here the extent to which the martensite-start temperature of the weld filler metal can be adjusted to mitigate residual stress distributions in ferritic steel welds has been investigated. Three single-pass groove welds were deposited by manual-metal-arc welding on 12 mm thick steel plates using filler metals designed to have different martensite-start temperatures. Their residual stress distributions were then characterised by neutron diffraction. It was found that a lower transformation temperature leads to a potentially less harmful stress distribution in and near the fusion zone. The experimental method is reported and the results are interpreted in the context of designing better welding consumables.

INTRODUCTION

Many major engineering failures occur due either to fatigue or environmentally-assisted cracking exacerbated by residual stresses introduced during welding. In assessing the integrity of an engineering structure it is necessary to estimate both the external or primary loads, as well as any secondary loading associated with residual stresses. The latter can have significant effects on the susceptibility of a material to degradation mechanisms such as fatigue and environmentally-assisted cracking. Residual stresses arise as a result of welding operations because they involve the deposition of molten filler metal and the localised input of intense heat. In the case of steels, the problem can be complicated by the fact that solid-state phase transformations occur during heating and cooling of the material. For example, in such a steel, low cooling rates might lead to the formation of ferrite

and pearlite in a diffusional phase transformation. On the other hand, more rapid cooling might induce martensite formed by a shear transformation. The significantly different displacements associated with these two mechanisms of phase change can have dramatically different consequences on the development of residual stress in the system as a whole [1-3].

The conventional way of coping with the prospect of high weld residual stresses is to reduce design stresses, or to conduct post weld heat treatments to relieve the residual stresses. An alternative approach for steels exploits displacive phase transformations to control the development of residual stresses. This is the focus of the current paper.

When austenite in steels transforms into plates of bainite or martensite, the phase change causes a deformation which is an invariant-plane strain consisting of a large shear on the habit plane and a dilatational strain normal to the plane. Each austenite grain can transform into 24 different crystallographic variants of the plates. If each variant occurs in equal measure the shears cancel so that the macroscopic shape deformation simply reflects the volume change. However, external stress can favour the formation of specific variants. This selectivity may counteract the build up of tensile stresses arising from the contraction of the weld as it cools. If, however, the transformation exhausts before cooling is complete then further contraction can lead once again to the build up of stresses until ambient temperature is achieved.

It is important therefore to tailor the transformation temperature of the filler alloy through judicious alloying such that the compensation process can be sustained to ambient temperature. In this way Ohta *et al*. [4, 5] and Wang *et al*. [6] were able to realize transformation induced stress-relief, and demonstrated a significant increase in the fatigue crack propagation resistance of weldments. In the present work weld filler materials have been designed with the stress compensating mechanism in mind but which are also tough, with the aim of improving performance in actual welded joints.

EXPERIMENTAL DETAILS

Filler Metals

Three filler metal compositions were chosen so as to have markedly different martensite-start (M_S) temperatures. The filler metal, OK75.78 is a commercially available electrode for which transformation should exhaust before ambient temperature is reached [7]. LTTE is a low M_S filler proposed by Wang *et al*. [6]. Finally, the filler designated "Series B" is an alternative formulation selected by the current authors. The compositions are summarised in Table 1.

Table 1: Approximate compositions of base plate and filler metals in wt. %.

Material	C	Si	Mn	Cr	Ni	Mo	Cu
Weldox 960	0.20	0.50	1.6	0.7	2.0	0.7	0.3
OK 75.78	0.05	0.19	2.0	0.4	3.1	0.6	-
LTTE	0.07	0.20	1.3	9.1	8.5	-	-
Series B	0.03	0.65	0.5	1.0	12.0	0.5	-

It is possible to estimate the bainite-start (B_S) and M_S temperatures for ferritic-martensitic filler metals using a computer program developed as part of the Materials Algorithm Project [8]. Details of the underlying principles for the software are available in the literature [9-11]. The B_S and M_S temperatures were estimated in this way for each of the filler alloys and they are summarised in Table 2. Bainite does not occur in the LTTE and Series B alloys which are martensitic. Note that the shape deformations due to bainite and martensite are essentially the same so for the present purposes it is only important to focus on the transformation temperatures [12].

Table 2: Estimates for B_S and M_S (ºC).

Parameter	OK75.78	LTTE	Series B
B_S	421	--	--
M_S	388	200	275

As expected, there are significant differences between the temperatures at which transformations can begin amongst the three alloys, ranging from 421 °C for OK75.78 to 200 °C for LTTE.

Satoh Tests on Filler Metals

Satoh tests [13, 14] were carried out to characterise the mechanical response of each alloy during cooling from the austenitic state. To do this, an unconstrained matchstick-shaped sample was austenitized by heating to 850 °C for 60 s, it was then rigidly fixed at its ends and allowed to cool at 10 $°C\,s^{-1}$ under this restraint whilst monitoring the stress.

Manufacture of Welded Plates

Three rectilinear plates ($375 \times 200 \times 12$ mm) were prepared from the high strength ferritic steel, Weldox 960. Along the center of each plate, a 5 mm deep Vee-groove was machined with an included angle of 60 °, into which a single weld bead was deposited using manual-metal arc welding. The consumables used were those listed in Table 1. The welding was undertaken in the down-hand position with a heat input between 1.1 and 1.4 kJ mm^{-1}. A preheat temperature of 125 °C was used and the plates were restrained by clamping during welding.

Stress Measurements in Welded Plates

Measurements of the residual stresses in the welded plates were conducted by neutron diffraction on the L3 spectrometer, which is part of the National Research Council of Canada facility at the NRU reactor, Chalk River. Monochromation of the neutron beam was achieved by diffraction from the $\{\overline{1}1\overline{5}\}$ planes of a germanium monochromator crystal at 92 °. The wavelength of the neutrons was 1.5651 ± 0.0001 Å from calibration measurements of the first four diffraction peaks using a nickel standard powder sample. With this wavelength, the {112} peaks from the ferritic and martensitic material in the welded plates could be observed at an angle of $2\theta \approx 84°$ which, being close to 90 °, provided optimal spatial resolution and avoided peak asymmetry arising as a result of axial divergence.

Positioning of the sample in the neutron beam was accomplished with an *XYZ* translation stage attached to a 360 ° rotational drive. With these drives, the sample could be positioned with an accuracy of 0.1 mm in *X, Y* and *Z* and 0.1 ° in rotational angle. Spatial resolution within the sample was achieved with cadmium slits inserted in the incident and diffracted beam paths. For all of the measurements, the slits were positioned within 20 mm of the sample surface to avoid penumbra effects.

Determination of the full strain tensor at each measurement position requires the measurement of the lattice strain in at least six independent directions. However, the orientation of one or more of the principal axes may be assumed from inspection of the geometry of the component. As is typical for measurements of this type, it was assumed that the principal axes were coincident with the axes of the plate. Whilst it may be reasonable to assume that one of the principal axes lies along the welding direction, the geometry of the weld fusion zone may be expected to lead to rotations of the principal axes from the transverse and normal directions in this plane. To test this assumption, additional measurements were made at an intermediate angle in this plane.

Measurements of the lattice strains were made in the plane perpendicular to the welding direction across the center of each plate (Figure 1). For measurements in the transverse and normal directions, the samples were orientated on the translation stage with the welds vertical. Slits 1 mm wide and 10 mm long were employed, providing a nominal gauge volume of $1 \times 1 \times 10$ mm in the sample. The use of these slits presupposes that the strains are invariant over the length of the slits. For the measurement of the longitudinal strains the samples were orientated with the transverse direction vertical and the welds parallel to the scattering vector. For these measurements, slits 1 mm wide and 2 mm long were used.

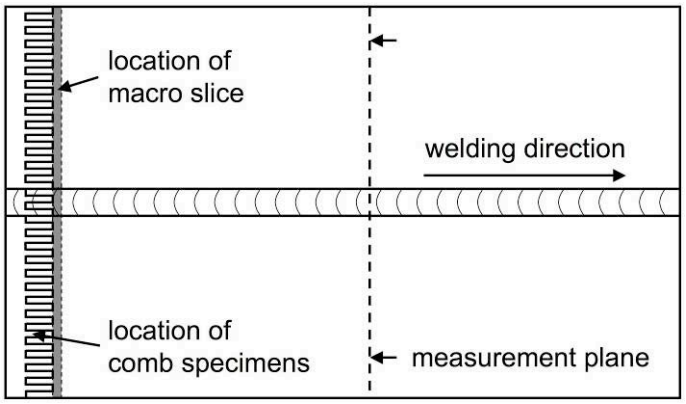

Figure 1: Schematic representation of welded plate showing location of reference combs, slice extracted for macrograph and location of measurement plane.

Determination of Strain-Free Lattice Spacings

To eliminate the effects of compositional variations on the lattice spacings, stress-free samples were cut from the weld so that reference lattice parameters could be determined. The samples were cut by electro-discharge machining from the last 30 mm of each welded plate as a series of combs with teeth 2 mm by 2 mm in section and 20 mm long (Figure 1). The dimensions of the teeth were chosen to allow the diffraction gauge volume to be fully immersed in the sample. The long direction of the teeth was aligned parallel with the welding direction in order to avoid incomplete stress relaxation as a result of stress

gradients in the plane perpendicular to the weld. This also provided maximum spatial resolution of lattice parameter variations in the transverse plane. Combs were extracted from each plate at depths of 1, 2.5, 4, 6, 8.5 and 11 mm from the top surface of the plate.

Metallography

Macrographs were prepared so that the measured residual stress distributions could be correlated with the different metallurgical zones in each of the welded plates. One 5 mm thick slice was removed from the end of each plate by electro-discharge machining (Figure 1). Each slice was then ground and polished to a 1 μm finish prior to etching in 2 % Nital for 15 seconds. The macrographs for each weld are shown in Figure 2. It can be seen from Figure 2 that the weld bead penetrations are close to 6 mm, equivalent to half the plate thickness. Whilst there are minor variations from one weld to another, the extent of the fusion zone and HAZ in each weld is similar, as the same nominal welding parameters were used in each case. The heat-affected zone (HAZ) reveals two distinct bands. An examination of the microstructure confirmed that the inner and darker band (in the case of OK75.78), which extends from the fusion line for approximately 2 to 3 mm, corresponds to the fully austenitized zone. The outer band appears lighter and comprises the partially austenitized region and over-tempered base metal. It would appear from Figure 2 that the over-tempered region of the heat-affected zone extends to the bottom surface of the plate in each sample. In the context of this study, the fully austenitized region within the HAZ is of greater interest as, in addition to the fusion zone, it will transform from austenite upon cooling. However, the transformation temperature within the HAZ will be determined by the local cooling rate and the composition of the parent material, rather than the composition of the fusion zone.

ANALYSIS OF RESIDUAL STRESS DATA

The measured diffraction peaks were fitted with a Gaussian function having a constant background. In this manner the Bragg angle, $\theta_{\{112\}}$, was determined point by point within the sample. The lattice spacings, $d_{\{112\}}$, were then obtained from the Bragg equation:

$$\lambda = 2d_{\{112\}} \sin\theta_{\{112\}} \quad (1)$$

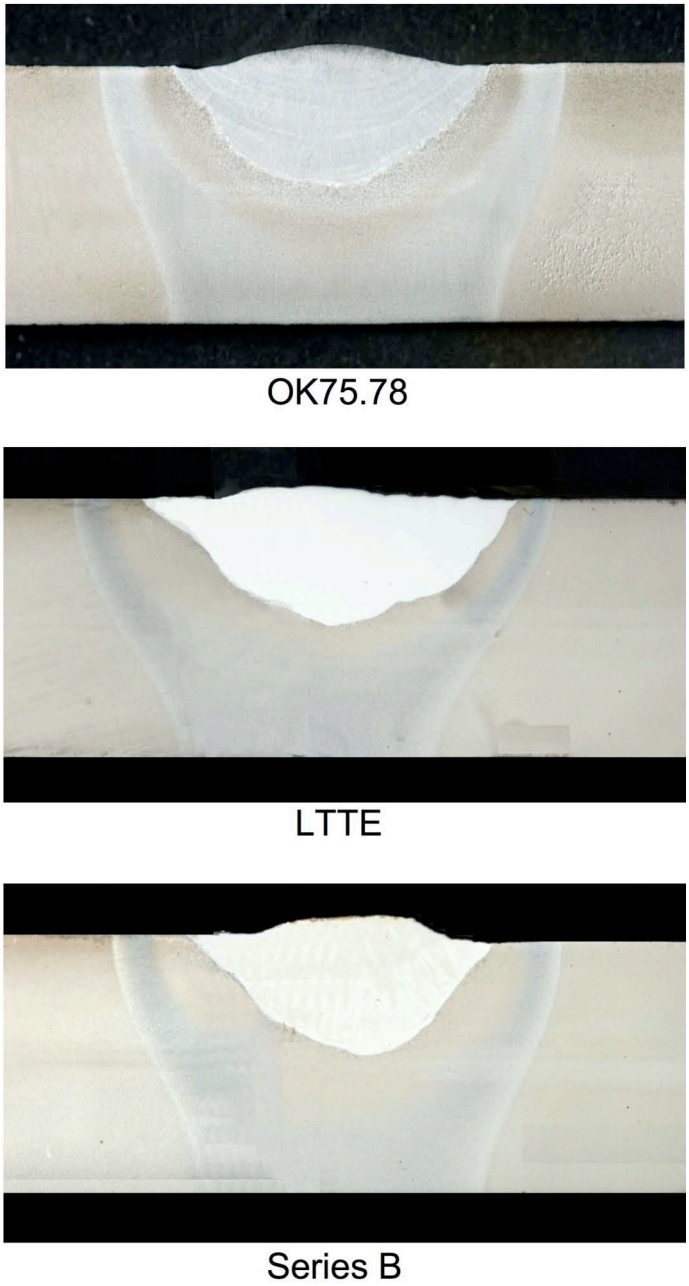

Figure 2: Macrographs through the 12 mm welded plates made with each of the filler metals. The extent of the fusion zone and HAZ is similar in each.

With these lattice spacings the corresponding strains, $\varepsilon_{\{112\}}$, were obtained with respect to the measured stress-free lattice parameter, d_0, corresponding to that location using:

$$\varepsilon_{\{112\}} = \left(d_{\{112\}} - d_0\right)/d_0 \quad (2)$$

The measured lattice strain is the resolved component of the strain, $\varepsilon_{\{112\}}$, on to the measurement direction:

$$\varepsilon_{\{112\}} = \sum_{all\ i,j} \varepsilon_{ij}\alpha_i\alpha_j \qquad (3)$$

where α_i and α_j are the direction cosines between the measurement direction and the principal axes. The principal strains can be acquired by matrix diagonalization so that the stresses may be obtained from:

$$\sigma_i = \frac{E_{\{112\}}}{(1+\nu_{\{112\}})}\varepsilon_i + \frac{\nu_{\{112\}}E_{\{112\}}}{(1+\nu_{\{112\}})(1-2\nu_{\{112\}})}\sum_{all\ j}\varepsilon_j \qquad (4)$$

where σ_i is the principal stress in the i direction and $E_{\{112\}}$ and $\nu_{\{112\}}$ are the plane specific Young's modulus and Poisson's ratio, respectively. In this work, we have assumed that the welding direction corresponds to one of the principal directions and, in the first instance, rather than evaluating the other principal stresses we have analysed stresses acting along the axes of the plates.

RESULTS AND DISCUSSION

Satoh Tests

The results of the Satoh tests are shown in Figure 3.

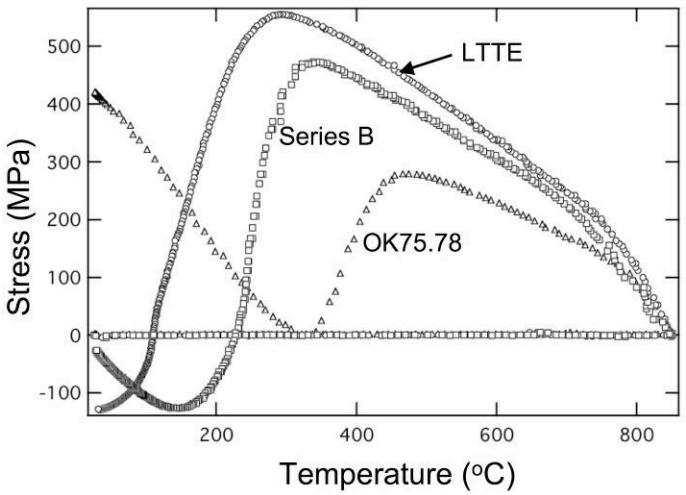

Figure 3: Results of Satoh tests on each of the weld filler metals cooling from 850 °C at 10 °C s^{-1}.

In the absence of phase transformations and given the constraint, the tensile stress is expected to increase monotonically with decreasing temperature. At a temperature that corresponds approximately to the expected B_S or M_S temperature for each alloy there is a reduction in the stress. The relatively high transformation temperature of OK75.78 results in the build up of stress once the transformation exhausts. In contrast, the transformation temperature of LTTE is sufficiently low for the transformation strain due to the martensitic transformation to overwrite the tensile stresses that had accumulated due to thermal contraction, and generate compressive transformation stresses at ambient temperature. Finally Series B, with its intermediate M_S temperature, is left with almost zero stress at ambient temperature.

Stress Measurements on Welded Plates

The results of the neutron diffraction measurements are shown in Figure 4. Each of the contour plots shows the longitudinal stresses that were measured over a cross-section of the weld corresponding to the mid-length position. The stress maps are superimposed upon the corresponding macrograph for each weld so that the features of the stress maps can be correlated with the different metallurgical zones. There was a significant level of noise in the as-calculated stresses; a symptom of the inherent variability associated with combining three strain measurements and the corresponding stress-free reference measurement needed at each point to infer the stress. As such, the stresses were averaged using a mirroring technique. That is to say that symmetry was assumed about the weld centerline (this was supported by the point to point measurements), and each calculated stress was averaged with the value at the corresponding mirror image location about the weld centerline. Thus, the results plotted in Figure 4 correspond to averaged values.

In the weld made with OK75.78, both the weld nugget and the underlying reaustenitized HAZ are expected to have transformed at high temperatures. Consequently, the stress contours in the HAZ are almost vertical, as if a full-penetration weld has been deposited. The level of stress both in the weld nugget and underlying region is low but the tensile stress increases with distance along the horizontal axis, with peak stresses of about 800 MPa located at about half the depth and in the HAZ. The domain in which the stress is greater than 600 MPa is large, with a width of just under 5 mm parallel to the horizontal axis.

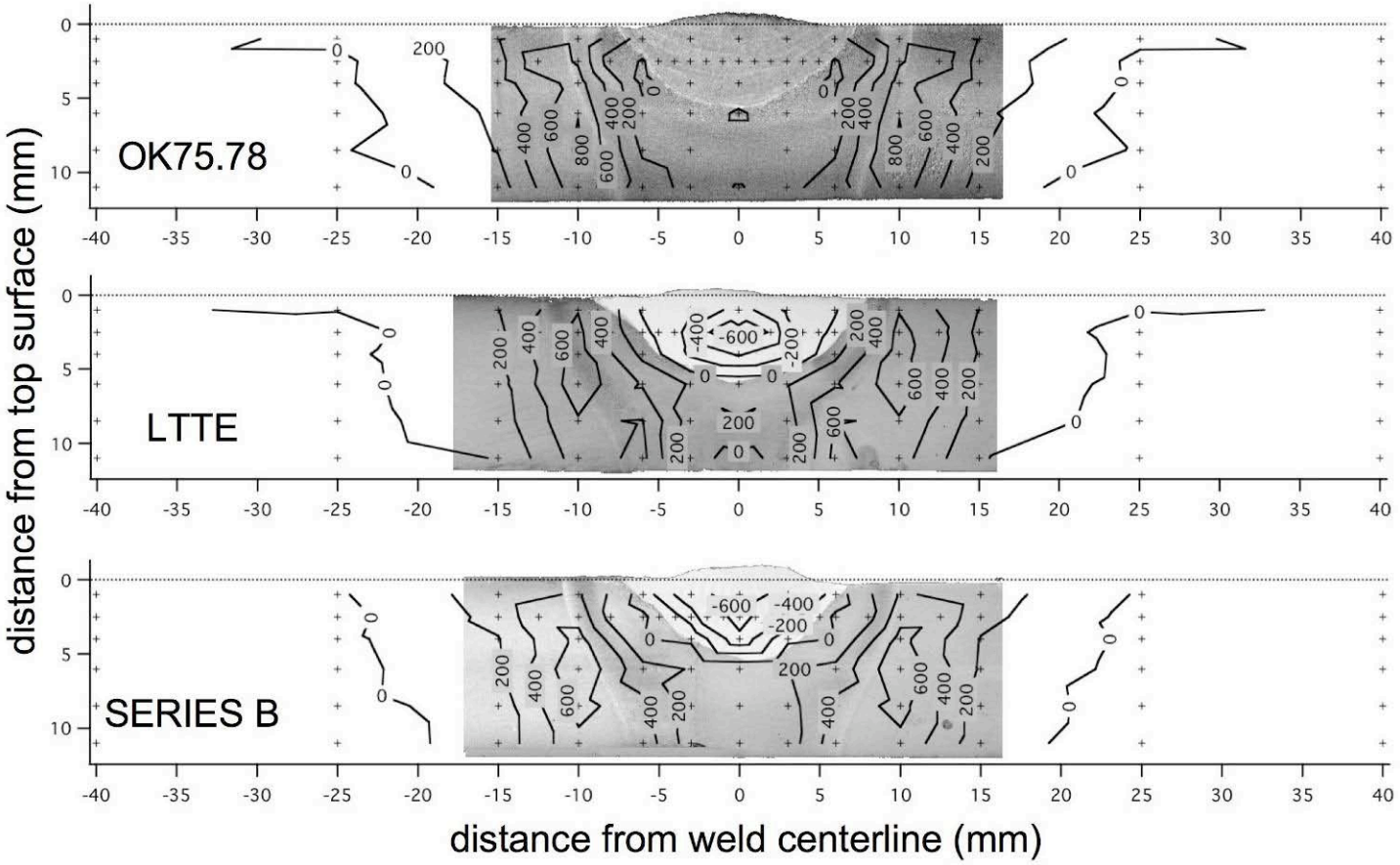

Figure 4: Longitudinal residual stresses estimated using neutron diffraction measurements at locations marked by crosses. For each weld, the stresses are superimposed on the corresponding macrograph.

Major differences are evident for the LTTE and Series B samples, both of which have low transformation temperatures compared with the plate material. There are major compressive stresses within the weld nuggets. To a depth of 5 mm, the stress contours within the HAZ closely follow the shape of the nugget, i.e., steeply inclined stress contours. This is in stark contrast to those in OK75.78. The phase change within the nugget has resulted in a large reduction of the tensile stresses within the adjacent HAZ up to the depth of 5 mm. The peak tensile stresses are much smaller than in OK75.78 and the regions within which they occur are also smaller.

In the regions under the nuggets of LTTE and Series B, the phase change occurs at a higher temperature than for the nugget itself. It is therefore possible for tensile stresses to arise in these regions. To a certain degree, the interpretation of the stress distributions in these regions is complicated by the fact that the residual stresses must balance over the weld section. Thus, in these regions it is possible that the stresses may not be explained solely in terms of the local transformation temperature.

The variation in longitudinal stress with distance from the weld centerline is shown again for each weld in Figure 5. Here each plot corresponds to a different depth below the top surface of the welded plate. The extent to which compressive stresses are induced in the weld nugget by the low transformation temperature filler metals is evident in the first two plots, which correspond to depths of 1 and 2.5 mm respectively.

Immediately under the weld nugget and close to the weld centerline, at depths of 6 and 8 mm, the stresses in the welds made with LTTE and Series B are more tensile than those for OK75.78. When the transformations are in progress within the fusion zone for the welds made with LTTE and Series B, the transformations in the adjacent HAZ regions will already have exhausted, since they occur at a higher temperature. Thus the

transformation strains in the fusion zone are likely to have exacerbated the accumulation of tensile stresses in the nearby HAZ. Further from the fusion zone, at a depth of 11 mm, the stresses with LTTE and Series B are once again lower than for OK7578. This may have resulted from the requirement to balance the larger tensile stresses generated closer to the weld nugget.

When the residual stresses at all depths are considered, it is evident that the LTTE and Series B alloys have been effective in reducing the build up of tensile stress across the HAZ. It is also possible that the observed compensation would have been greater and more uniform if full penetration welds had been made. The potential for mitigation of welding residual stresses in multipass welds using low transformation temperature filler metals thus offers exciting opportunities for future work.

CONCLUSIONS AND FUTURE WORK

- In all cases solid-state phase transformations have reduced the tensile residual stresses that would be expected in and around the fusion zone relative to welds in which transformations do not take place, being essentially zero in the OK75.78 weld and compressive in welds made with the lower transformation temperature filler metals.
- The low-transformation-temperature filler metals also resulted in reductions in the peak tensile residual stresses in the HAZ for the case of a single weld pass in a Vee-groove on a 12 mm thick ferritic steel plate.
- Further work is required to understand how the selection of a low-transformation-temperature filler metal may provide benefits in multi-pass welds where, for many weld passes, the HAZ will reside in previously deposited weld metal.
- Phase transformations can have very large effects on residual stress distributions, so models for welding residual stress development in ferritic steels will need to account for solid-state phase transformations.

ACKNOWLEDGMENTS

The authors would like to acknowledge the Worshipful Company of Ironmongers for financial support to help with travel to Canada. HJS would like to thank the Engineering and Physical Sciences Research Council for the provision of a financial grant, while JAF would like to acknowledge support from Rolls-Royce Naval Marine.

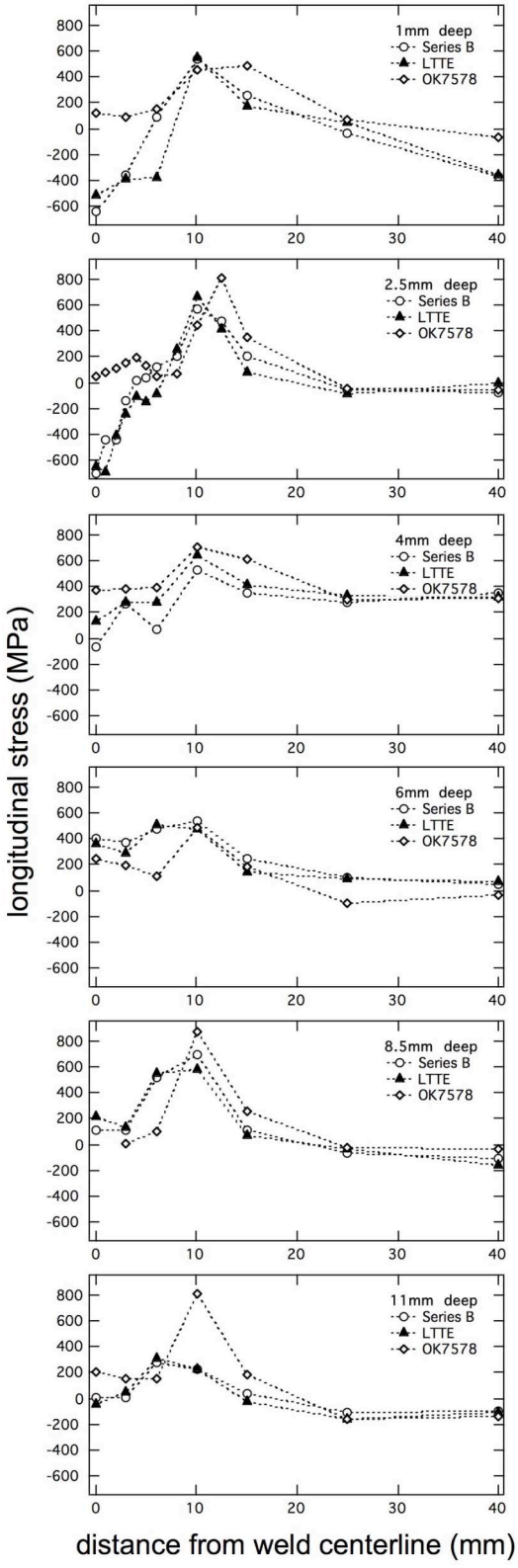

Figure 5: Variation in longitudinal stress with distance from weld centerline at different depths within each welded plate.

REFERENCES

[1] H.K.D.H. Bhadeshia: "Developments in Martensitic and Bainitic Steels – Role of the Shape Deformation", *Materials Science and Engineering A*, **378** (1-2), 34-39, 2004.

[2] P.J. Withers and H.K.D.H. Bhadeshia, "Overview – Residual Stress Part 1 – Measurement Techniques", *Materials Science and Technology*, **17** (4), 355-365, 2001.

[3] P.J. Withers and H.K.D.H. Bhadeshia, "Overview – Residual Stress Part 2 – Nature and Origins", *Materials Science and Technology*, **17** (4), 366-375, 2001.

[4] A. Ohta, N. Suzuki, Y. Maeda, K. Hiraoka and T. Nakamura: "Superior Fatigue Crack Growth Properties in Newly Developed Weld Metal", *International Journal of Fatigue*, **21**, S113-S118, 1999.

[5] A. Ohta, K. Matsuoka, N.T. Nguyen, Y. Maeda and N. Suzuki: "Fatigue Strength Improvement of Lap Joints of Thin Steel Plate Using Low-Transformation-Temperature Welding Wire", *Welding Journal*, **82** (4), 78S-83S, 2003.

[6] W.X. Wang, L.X. Huo, Y.F. Zhang, D.P Wang and H.Y. Jing: "New Developed Welding Electrode for Improving the Fatigue Strength of Welded Joints", *Journal of Materials Science & Technology*, **18** (6), 527-531, 2002.

[7] M. Lord, Ph.D. Thesis, University of Cambridge, 1998.

[8] www.msm.cam.ac.uk/map/steel/steelprog.html

[9] H.K.D.H. Bhadeshia: "Thermodynamic Analysis of Isothermal Transformation Diagrams", *Metal Science*, **16** (3), 159-165, 1982.

[10] H.K.D.H. Bhadeshia: "*Bainite in Steels*", *Institute of Materials*, London, 1-410, 2001.

[11] S. M. Hodson: "MTDATA-Metallurgical and Thermochemical Databank", *National Physical Laboratory*, Teddington, UK, 1989.

[12] H.K.D.H. Bhadeshia: "Some Phase Transformations in Steels", *Materials Science and Technology*, **15** (1), 22-29, 1999.

[13] K. Satoh: "Transient Thermal Stresses of Weld Heat-Affected Zone by Both-Ends-Fixed Bar Analogy", *Transactions of the Japan Welding Society*, **3** (1), 125-134, 1972.

[14] K. Satoh: "Thermal Stresses Developed in High-Strength Steels Subjected to Thermal Cycles Simulating Weld Heat-Affected Zone", *Transactions of the Japan Welding Society*, **3** (1), 135-142, 1972.